A DFT Study of Stannane Dehydrocoupling Catalyzed by Cp_2LaH

Christophe Raynaud,[†] Lionel Perrin,[†,‡] and Laurent Maron*,[†]

Laboratoire de Physique Quantique, IRSAMC, Université Paul Sabatier and CNRS (UMR 5626), 118 Route de Narbonne, 31064 Toulouse Cedex, France, and Protéines Membranaires Transductrices d'Energie, URA 2096 du CNRS, DSV/DBJC/SBFM, CEA-Saclay, 91191 Gif-sur-Yvette Cedex, France

Received December 12, 2005

All the pathways leading to bis-stannane and regeneration of the catalyst Cp_2LaH ($Cp = \eta^5$-C_5H_5) for the stannane SnH_4 have been computed using the DFT (B3PW91) method. In all cases, the reaction is at least a two-step process with a common first step, which is the Sn−H activation of the stannane, leading to the hydrostannyl complex Cp_2LaSnH_3. From a pure thermodynamic point of view, the overall process is found to be exergonic by 9.3 kcal·mol^{-1}. Since the most stable product of the energy profile is the intermediary hydrostannyl complex, the second step, which corresponds to Sn−Sn coupling, is endergonic. This explains the relatively low turnover, found experimentally, for the homocoupling of stannane into bis-stannane. This overall process is in agreement with the experiment made on hafnium complexes, where the intermediary hydrostannyl compounds have been isolated and characterized. From a kinetic point of view, the second reaction step is proposed to occur through a direct SnH_3 transfer of the hydrostannyl to the incoming stannane rather than stannylene or stannylenoide insertion into the incoming stannane.

Introduction

From a chemical point of view, achieving the dehydropolymerization of stannane is of interest since the formed polystannanes exhibit peculiar optical and electronic properties.[1−3] Moreover, the related possibility of catalytically obtaining these polymers, using for example transition metal- or lanthanide-based complexes, is also of particular interest. Two catalysts developed by Tilley's group have been reported in the literature.[4−7] The authors have shown that the zirconocene $CpCp^*Zr[Si(SiMe_3)_3]Me$[4,5] or $CpCp^*Hf(H)Cl$[6] complexes ($Cp = \eta^5$-C_5H_5 and $Cp^* = \eta^5$-C_5Me_5) are very active catalysts toward the dehydropolymerization process. To better understand and to further control the polymerization process, the knowledge of the reaction mechanism is crucial. Neale et al.[6] have reported some mechanistic information in the hafnium case for the secondary stannane Mes_2SnH_2 (Mes = 2,4,6-trimethylphenyl) dehydropolymerization. In particular, the authors have been able to isolate and characterize the hydrostannyl intermediate $CpCp^*Hf(SnHMes_2)Cl$, which was speculated in the zirconium case. This indicates that the first step of the process is a Sn−H activation. For the latter complex, no α-agostic interaction has been observed. The authors have suggested that bis-stannane is formed, in a second step, by insertion of stannylene into a Sn−H bond of a second incoming stannane molecule. The stannylene is obtained by α-elimination from the hydrostannyl intermediate.[6,7] Indeed, the thermal decomposition of the hydrostannyl complex led, after a course of 3 days, to the hydride and some cyclic species derived from the oligomerization of the stannylene. In addition the stannylene has been trapped in the presence of a trapping agent. Moreover, in the presence of H_2, it has been possible to show that the reaction of the hydride with the stannane is reversible. After 2 days, 92% of the formed hydrostannyl is converted to the hydride and 21% of bis-stannane is formed. For this first step of the reaction, the authors have performed a kinetic study in a temperature range (0.7−33.2 °C) that leads to an activation enthalpy of 7.4 kcal·mol^{-1} and an activation entropy of −42 eu. For the second step, the authors have ruled out the H/Sn exchange process between the hydrostannyl and the incoming stannane based on steric problems.

Since the past few years, theoretical mechanistic investigations of reactions involving lanthanide complexes have been computationally accessible[8−12] mainly due to the use of effective core potentials (ECP) that include the inert 4f electrons in core.[13−15] Thus, some combined experimental and theoretical studies have shown that σ-bond activation reactions catalyzed by lanthanide complexes could occur via the formation of unsaturated species. This was mainly observed in the case of C−F activation. Recently, Maron et al.[16] have shown that in the process of C−F activation of fluoroarenes unsaturated species such as benzyne derivatives were formed and experimentally trapped. In the same way, Wekerma et al.[17] have shown that the reaction of hydrofluoromethane with Cp'_2CeH formed

* Corresponding author. E-mail: Laurent.Maron@irsamc.ups-tlse.fr.
[†] Laboratoire de Physique Quantique, Université Paul Sabatier and CNRS.
[‡] Protéines Membranaires Transductrices d'Energie, URA 2096 du CNRS.

(1) Braunstein, P.; Morise, X. *Chem. Rev.* **2000**, *100*, 3541.
(2) Pitt, C. G. In *Homoaromatics Rings, Chains and Macromolecules of Main-Group Elements*; Rheingold, A. L., Ed.; Elsevier Scientific: New York, 1977.
(3) Takeda, K.; Shiraishi, K. *Chem. Phys. Lett.* **1992**, *195*, 121.
(4) Imori, T.; Lu, V.; Hui, C.; Tilley, T. D. *J. Am. Chem. Soc.* **1995**, *117*, 9931.
(5) Lu, V.; Tilley, T. D. *Macromolecules* **1996**, *29*, 5763.
(6) Neale, N. R.; Tilley, T. D. *J. Am. Chem. Soc.* **2002**, *124*, 3802.
(7) Neale, N. R.; Tilley, T. D. *J. Am. Chem. Soc.* **2005**, *127*, 14745.
(8) Maron, L.; Eisenstein, O. *J. Am. Chem. Soc.* **2001**, *123*, 1036.
(9) Maron, L.; Perrin, L.; Eisenstein, O. *J. Chem. Soc., Dalton Trans.* **2002**, 534.
(10) Maron, L.; Perrin, L.; Eisenstein, O. *J. Chem. Soc., Dalton Trans.* **2003**, 4313.
(11) Perrin, L.; Maron, L.; Eisenstein, O. *Inorg. Chem.* **2002**, *41*, 4355.
(12) Sherer, E. C.; Cramer, C. J. *Organometallics* **2003**, *22*, 1682.
(13) Dolg, M.; Fulde, O.; Küchle, W.; Neumann, C.-S.; Stoll, H. *Chem. Phys.* **1991**, *94*, 3011.
(14) Dolg, M.; Stoll, H.; Preuss, H. *Theor. Chim. Acta* **1993**, *85*, 441.
(15) Dolg, M.; Stoll, H.; Savin, A.; Preuss, H. *Theor. Chim. Acta* **1989**, *75*, 173.
(16) Maron, L.; Wekerma, E. L.; Perrin, L.; Eisenstein, O.; Andersen, R. A. *J. Am. Chem. Soc.* **2005**, *127*, 279.

10.1021/om051060m CCC: $33.50
Publication on Web 05/18/2006

Chart 1. Definition of α and β Positions in the Four-Center Transition State

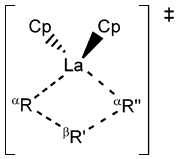

Cp'_2CeF in a two-step process ($Cp' = \eta^5$-1,3,4-$tBu_3C_5H_2$), where the second step corresponds to a carbenoide insertion into a H−H bond. Thus, the possibility of generalizing this type of mechanism to other kinds of molecules, involving for example the Sn atom, makes this study attractive from a theoretical point of view. In this paper, all pathways leading to the bis-stannane formation have been theoretically investigated using lanthanide catalysts.

The main difference between alkane and stannane (or silane) is that in the case of alkane the C−C coupling has been found to be kinetically unfavorable.[9,18] Alternatively, a recent study of the dehydrocoupling process of primary silanes[19] has concluded that this process was occurring through a Si−H activation and a subsequent H/Si exchange. This was in agreement with the previous theoretical study on the Si−H activation of SiH_4 by lanthanocene,[11] since both α and β positions (see Chart 1 for the definition of these positions) in the four-center transition state are accessible to Si. Thus, it is of interest to see how different the reaction paths can be in the case of stannane.

In this paper, the reaction pathways for the stannane dehydrocoupling reaction catalyzed by Cp_2LaH, used as a generic model of metallocene hydride, have been computed for the stannane SnH_4 using DFT methods. It should be noticed that SnH_4 is sterically very different from the secondary stannane used by Neale et al.[6] (Mes_2SnH_2). However, the steric effects associated with the two mesityl substituents (which have been modelized by phenyl) will be discussed only with regard to the thermodynamics of the first step. Moreover, the metallic fragment is also less encumbered than the corresponding hafnium one; the charge is also different, and this can lead to different results from experiment. All the free-energy profiles have been computed at 298.15 K. Three different pathways leading to Sn−Sn coupling have been computed and will be discussed. The first one is based on an H/Sn exchange, whereas the two other pathways imply a stannylene (or stannylenoide) formation.

Computational Details

In previous studies,[8−11] we have shown that large core pseudopotentials from the Stuttgart group[13−15] allow a good treatment of the lanthanide center. The lanthanide center has been treated with the optimized basis set augmented by a set of polarization functions (namely an f function with an exponent α equal to 1.000). Tin atoms have been represented with an ECP[20] and the adapted basis set, augmented with a set of d polarization functions with an exponent equal to 0.284.[21] The carbon and hydrogen atoms are treated with an all-electron double-ζ, 6-31G(d,p)[22] basis set. All the calculations have been carried out with the Gaussian 98 suite of programs[23] at the DFT level using the B3PW91[24,25] hybrid functional. Geometry optimizations have been performed without any symmetry constraints. Vibrational analysis has been done using analytic determination of the frequencies (harmonic approximation) in order to estimate the thermodynamic and kinetic data at 298.15 K. The intrinsic reaction coordinate[26] (IRC) has been followed to confirm that transition states connect to reactants and products.

Results and Discussion

***β*-Pathway: A Two-Step Pathway with Sn−H Activation and H/Sn Exchange.** Let us start by considering the pathway implying two successive Sn−H bond activations. The calculated pathway for the entire reaction is presented in Figure 1. As seen in Figure 1, the total reaction is calculated to be exergonic by 9.3 kcal·mol^{-1} and the higher activation barrier is found to be 9.2 kcal·mol^{-1}. This leads to a thermodynamically and kinetically favorable reaction.

First Step: Hydrostannyl Formation, $Cp_2LaH + SnH_4 \rightarrow Cp_2LaSnH_3 + H_2$. For the first step of the reaction, which corresponds to the formation of hydrostannyl **5**, the reaction is calculated to be exergonic by 18.3 kcal·mol^{-1}, with an activation barrier of 9.2 kcal·mol^{-1} (−2.9 kcal·mol^{-1} in enthalpy with respect to the reactants). The difference from the value reported by Neale and Tilley[6] is clearly associated with the difference of the metallic fragment and the lack of steric hindrance of the stannane with respect to the bismesityl one used experimentally. The reaction starts with the formation of a σ-adduct of SnH_4 from the reactant Cp_2LaH **1**. This adduct **3** is calculated to be destabilized by 8.2 kcal·mol^{-1} with respect to the free reactants. This destabilization is mainly due to the loss of translational and rotational entropy of the free stannane.[27] This adduct connects to transition state **2**.

At the transition state, Sn is at the α position in the four-membered ring (see Chart 1 for the definition of α and β positions). The activation barrier is found to be 9.2 kcal·mol^{-1} relative to the separated reactants but only 1.0 kcal·mol^{-1} relative to the adduct **3**. Thus, **3** efficiently prepares the transition state. The transition state **2** then connects to an H_2 adduct **4**, which is stabilized by 10.4 kcal·mol^{-1} relative to the separated reactants. Then the release of H_2 by **4**, yielding the intermediate complex $Cp_2La(\eta^2$-$SnH_3)$, is thermodynamically favorable by 7.9 kcal·mol^{-1}. This exergonicity essentially originates from the gain in rotational and translational entropy. It should be noticed that two different isomers could have been optimized for the hydrostannyl complex. The first one, labeled **5**, is lower in energy by 4.5 kcal·mol^{-1} than the other one, labeled **5′**. The difference between these two complexes is an interaction

(17) Wekerma, E. L.; Messines, E.; Maron, L.; Perrin, L.; Eisenstein, O.; Andersen, R. A. *J. Am. Chem. Soc.*, submitted.
(18) Folga, E.; Ziegler, T. *Can. J. Chem.* **1992**, *70*, 333.
(19) Perrin, L.; Eisenstein, O.; Maron, L. *J. Chem. Soc., Dalton Trans.*, submitted.
(20) Bergner, A.; Dolg, M.; Küchle, W.; Stoll, H.; Preuss, H. *Mol. Phys.* **1993**, *80*, 1431.
(21) Trinquier, G. *J. Chem. Soc., Faraday Trans.* **1993**, *89*, 775.
(22) Hariharan, P. C.; Pople, J. A. *Theor. Chim. Acta* **1973**, *28*, 213.
(23) Frisch, M. J.; Trucks, G. W.; Schlegel, H. B.; Scuseria, G. E.; Robb, M. A.; Cheeseman, J. R.; Zakrzewski, V. G.; Montgomery, J. A.; Stratmann, R. E.; Burant, J. C.; Dapprich, S.; Millam, J. M.; Daniels, A. D.; Kudin, K. N.; Strain, M. C.; Farkas, O.; Tomasi, J.; Barone, V.; Cossi, M.; Cammi, R.; Mennucci, B.; Pomelli, C.; Adamo, C.; Clifford, S.; Ochterski, J.; Petersson, G. A.; Ayala, P. Y.; Cui, Q.; Morokuma, K.; Malick, D. K.; Rabuck, A. D.; Raghavachari, K.; Foresman, J. B.; Cioslowski, J.; Ortiz, J. W.; Baboul, A. G.; Stefanov, B. B.; Liu, G.; Liashenko, A.; Piskorz, P.; Komaromi, I.; Gomperts, R.; Martin, R. L.; Fox, D. J.; Keith, T.; Al-Laham, M. A.; Peng, C. Y.; Nanayakkara, A.; Gonzalez, C.; Challacombe, M.; Gill, P. M. W.; Johnson, B. G.; Chen, W.; Wong, M. W.; Andres, J. L.; Head-Gordon, M.; Replogle, E. S.; Pople, J. A. *Gaussian 98*, A.9; Pittsburgh, PA, 1998.
(24) Becke, A. D. *J. Chem. Phys.* **1993**, *98*, 5648.
(25) Burke, K.; Perdew, J. P.; Yang, W. *Electronic Density Functional Theory: Recent Progress and New Directions*; Dobson, J. F., Vignale, G., Das, M. P., Eds.; 1998.
(26) Fukui, K. *J. Phys. Chem.* **1970**, *74*, 4161.
(27) Watson, L.; Eisenstein, O. *J. Chem. Educ.* **2002**, *79*, 1269.

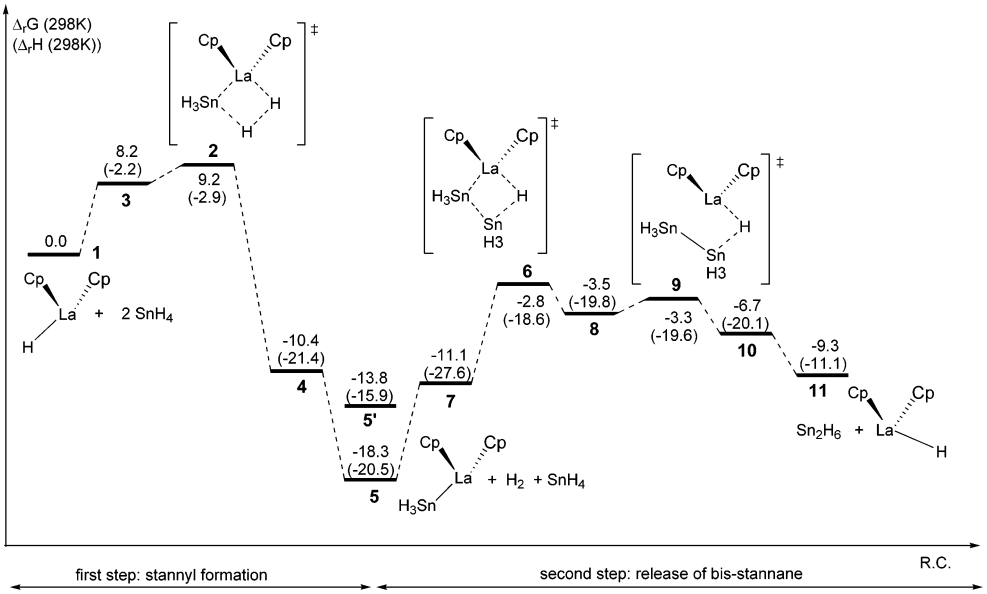

Figure 1. Calculated reaction pathway for the SnH_4 deshydropolymerization process. The free energies are given at 298 K, and the enthalpy values are in parentheses.

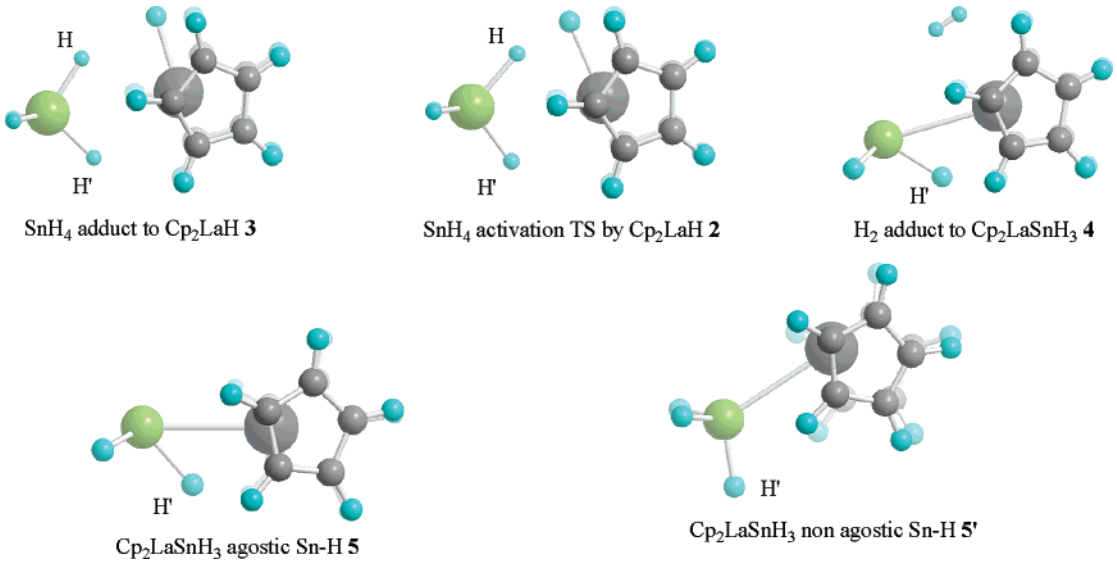

Figure 2. Optimized structures for the Sn−H activation reaction.

between La and a Sn−H bond (α-agostic interaction), observed in **5**. The strength of this interaction could be estimated as 4.5 kcal·mol^{-1}. The overall driving force of this reaction relies on the strength of the H−H bond (∼104 kcal·mol^{-1})[28] with respect to the Sn−H one (∼74 kcal·mol^{-1}).[28] Hence, if we do not take into account the α-SnH-agostic interaction, the La−H bond is stronger than the La−Sn bond by ∼16 kcal·mol^{-1}. This balance decreases to ∼12 kcal·mol^{-1} when considering the agostic interaction. Before, analyzing the energetic results on the second step of the process, let us discuss the geometry of the stationary point optimized in this first step. The geometries are presented in Figure 2 and Table 1.

In **3**, the stannane is oriented in such a way that two hydrogens, labeled H(Sn) and H′(Sn) in Table 1, are pointing toward the metal center. H(Sn) is the flying hydrogen that will form H_2 while reacting with the hydride, and H′(Sn) interacts in an agostic way. A NBO analysis[29] of this adduct shows that Sn is highly positively charged (+0.84), whereas the two hydrogen atoms are negatively charged, respectively −0.21 for H(Sn) and −0.27 for H′(Sn). Thus, it could be noticed at this stage that SnH_4 is interacting in an electrostatic way with the metal and that no interaction between La and Sn could be observed. This is in agreement with the fact that the C_3 axis of the remaining SnH_3 is oriented in the direction of the flying hydrogen. According to the charge analysis and the optimal charge distribution at the TS proposed in refs 30−32, the electronic changes needed to reach the TS should be important.

Table 1. Selected Distances of the Stationary Points of the First Step (Sn−H Activation of SnH_4 by Cp_2LaH)

	3	**2**	**4**	**5**	**5′**
La−H (Å)	2.15	2.16	2.70		
La−Sn (Å)	3.62	3.43	3.22	3.22	3.32
La−H(Sn) (Å)	2.80	2.51	3.30		
La−H′(Sn) (Å)	2.92	2.89	2.43	2.43	4.35
H(Sn)···H (Å)	2.33	1.60	0.76		
H′−Sn−H (deg)	109	107	98	97	101

(28) Frederikse, H. P. R.; Lide, D. R. *CRC Handbook of Chemistry and Physics*, 78 ed.; CRC Press: Boca Raton, 1997.

(29) Reed, A. E.; Curtiss, L. A.; Weinhold, F. *Chem. Rev.* **1988**, *88*, 899.

This seems not to be coherent with the small energy change obtained (this will be discussed in the next paragraph).

The geometry of the transition state **2** is very close to the one obtained for the stannane adduct **3**, as seen from Table 1. Indeed, the lanthanum hydride bond length is not much elongated (0.01 Å) with respect to the adduct. The stannane came closer to the metal center in order to lead to a shorter distance between the flying hydrogen and the hydride (1.60 Å vs 2.33 Å in the adduct). On the other hand, this sliding has not changed the orientation of the C_3 axis of the SnH_3, which is still oriented toward the flying hydrogen H(Sn). Thus, these small geometrical changes explain the small energy difference between the transition state and the adduct **3**. This is also confirmed by a NBO analysis on the transition state **2**, showing that no important electronic changes have occurred between the adduct and the transition state. Indeed, the charges of H(Sn) and H′(Sn) are almost the same as in the adduct (respectively −0.20 and −0.28, compared to −0.21 and −0.27). The charge on Sn has decreased to +0.75, but no interaction could be observed between La and Sn, essentially due to electrostatic repulsion. Thus, this transition state cannot be clearly viewed as a metathesis transition state, but rather as an acido-basic reaction in the field of the metal center. This transition state is stabilized by a nucleophilic assistance of H′(Sn), which interacts with the metal center. It should be noticed that the charges obtained are in agreement with the lower electronegativity of Sn than H.

The geometrical parameters of the H_2 adduct **4** are classic for an adduct in the lanthanide case. The H_2 bond is not activated, and one is not expecting a strong interaction between H_2 and the metal center. On the other hand, for complexes **2** and **3**, no interaction between La and Sn could have been observed. Thus, let us focus on the "La−Sn" bond. As can be seen from Table 1, the La−Sn distance has been reduced to 3.22 Å, but at the same time, the La···H′(Sn) distance has decreased from 2.89 Å at the transition state **2** to 2.43 Å in **4**. Moreover, within the SnH_3 ligand, the angle H′−Sn−(other H) is very acute (98°), which is in agreement with an interaction between H′ and the metal center. It should be noticed that this angle has been reduced by roughly 10° with respect to **2**. Thus, it seems that the interaction between SnH_3 and La is mainly through H′ rather than Sn. This is also confirmed by the fact that the C_3 axis of SnH_3 is not pointing toward the metal center and by a NBO analysis indicating that Sn is still positively charged (+0.13, which is much less than at the transition state, +0.75) and that H′ is negatively charged (−0.41, which is much than at the transition state, −0.27).

The release of H_2 can connect to two different minima, labeled **5** and **5′**. In **5**, as seen from Figure 2 and Table 1, the interaction between H′ and La is still observed. On the other hand, in **5′**, the interaction is not present. The stabilization of **5** corresponds more or less to the standard value of 8 kcal·mol^{-1} for the gain of translational entropy,[27] whereas the stabilization is lower in **5′**, 3.4 kcal·mol^{-1}. Thus, one is expecting that the geometrical parameters in **5** will be close to those in **4** and rather different from those in **5′**. This is in agreement with the results presented in Table 1. In particular, it should be noticed that the La−Sn distance in **5′** is longer than in **5** by 0.1 Å. On the other hand, as can be seen in Figure 2, the C_3 axis in **5′** is oriented toward the metal center, whereas in **5** this axis has the same orientation as in **4**. A NBO analysis performed on the two isomers shows that in **5** Sn is positively charged (+0.11) and H′ negatively charged (−0.41), whereas in **5′** Sn is marginally negatively charged (−0.004). Thus, in the latter, the electrostatic interaction between the SnH_3 ligand and the metallic fragment will be lesser than in **5**, leading to a less stable isomer. The stability of the hydrostannyl complex with respect to the reactants is in agreement with experimental observation. However, from the experimental point of view, Neale et al.[6] have reported that no interaction between the metal center and the Sn−H bond could have been observed. It seems to be different in the lanthanum case than in the hafnium one, since the stabilization is rather important (4.5 kcal·mol^{-1}). To check the possible influence of the stannane hindrance, a calculation on the thermodynamics of this first step with SnH_2Ph_2 has been performed. The two hydrostannyl isomers have been optimized, and the obtained geometries are presented in Figure 3. The formation of the agostic hydrostannyl complex from Cp_2LaH and SnH_2Ph_2 is calculated to be exergonic by 18.8 kcal·mol^{-1}. This value is in excellent agreement with the value of 18.3 kcal·mol^{-1} obtained in the case of SnH_4. This agostic complex is found to be more stable than the nonagostic one by 8.5 kcal·mol^{-1}, which is 4 kcal·mol^{-1} more than with SnH_4. Thus, a more bulky stannane increases the difference between **5** and **5′**, and thus, the difference seen in the experiment is due not only to the steric hindrance of the stannane but also to the difference of the metallic fragment. Indeed, the metal center in [CpCp*Hf(SnHMes$_2$)Cl] is octavalent; therefore the establishment of an α-SnH-agostic interaction would preliminary require decoordination of the chloride ligand. Such an agostic interaction would be persistent in time if it is stronger than the bonding of chloride, which is most unlikely. In the lanthanum case, complex **5** is neutral and the lanthanum center in already octavalent; hence the loss of this interaction disfavors the stabilization of the metal center. Finally, according to our computational results, SnH_4 is a rather good model for investigating the reactivity of the stannane.

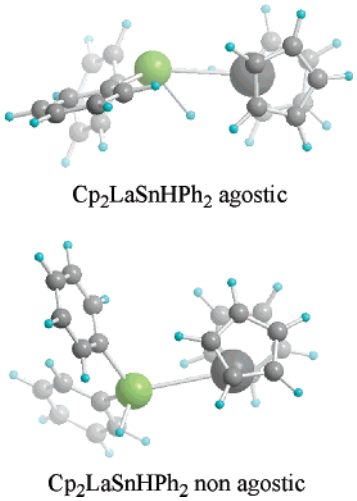

Figure 3. Geometry of the hydrostannyl complexes with phenyl groups.

On the basis of this validation of our model, let us investigate the second step of the reaction and the formation of the bis-stannane.

Second Step: Bis-Stannane Formation by Means of H/Sn Exchange from Hydrostannyl, $Cp_2LaSnH_3 + SnH_4 \rightarrow Cp_2LaH + Sn_2H_6$. Let us focus now on the second part of the free-energy profile presented in Figure 1, which corresponds

(30) Rabaâ, H.; Saillard, J. Y.; Hoffmann, R. *J. Am. Chem. Soc.* **1986**, *108*, 4327.
(31) Saillard, J. Y.; Hoffmann, R. *J. Am. Chem. Soc.* **1984**, *106*, 2006.
(32) Thompson, M. E.; Baxter, S. M.; Bulls, A. R.; Burger, B. J.; Nolan, M. C.; Santarsiero, B. D.; Schaefer, W. P.; Bercaw, J. E. *J. Am. Chem. Soc.* **1987**, *109*, 203.

to the reaction of a stannane molecule on the hydrostannyl complex to form the bis-stannane. First of all, it should be noticed that all the stationary points of this step are found to be below the reference, which has been chosen to be Cp_2LaH and two molecules of SnH_4. Thus, this reaction is not the rate-determining step. However, the reaction is calculated to be endergonic by 9.0 kcal·mol^{-1}, with an activation barrier of 15.5 kcal·mol^{-1}. This reaction seems not to be very productive, and this could be related to the fact that only 31% conversion into bis-stannane is experimentally observed after reaction of the entire amount of stannane. One can conclude that, if this step represents the experimental mechanism, it controls the turnover of the stannane into bis-stannane and that the control is mostly thermodynamic.

The reaction starts with the formation of a σ-adduct of stannane **7** from the hydrostannyl **5**. This adduct is found to be destabilized with respect to the free molecules by 7.2 kcal·mol^{-1}. This is slightly less than in the case of the adduct **3**. However, as in **3**, this destabilization is mainly due to the loss of entropy. Adduct **7** connects to the transition state **6**, where the incoming Sn atom is at the β position in the four-membered ring. The activation barrier is calculated to be 15.5 kcal·mol^{-1} relative to the hydrostannyl complex **5** and 8.3 kcal·mol^{-1} relative to the adduct **7**. Thus, it is possible to conclude that the adduct **7** does not efficiently prepare the transitions state and that energy-demanding changes are necessary to reach **6**. **6** connects to the complex **8**, which is a hypervalent complex of $Sn_2H_7^-$. This complex is found to be marginally stabilized with respect to the transition state **6** by 0.7 kcal·mol^{-1}. A similar behavior has already been reported in the litterature in the case of silane complexes by the group of Sabo-Etienne[33] on ruthenium chemistry and by Perrin et al.[19] on the deshydrocoupling of silane. This hypervalent complex is stabilized by a secondary interaction between Sn−H and the metal. This secondary interaction was defined as a SISHA interaction by the group of Sabo-Etienne.[33] Thus, to release the bis-stannane, it is necessary to reach another transition state, **9**, which is very close in energy to the hypervalent complex (0.2 kcal·mol^{-1} higher in energy). The secondary interaction is broken at this stage, and **9** evolves to the classical bis-stannane adduct **10**. This adduct is stabilized by 3.4 kcal·mol^{-1} with respect to the transition state **9**. From this adduct **10**, it is possible to regenerate the catalyst Cp_2LaH and to form bis-stannane **11**. This release is marginally exergonic (2 kcal·mol^{-1}) since the gain in entropy is small due to the size of the bis-stannane. Like in the first step of the process, let us analyze the geometry of the stationary points. The optimized geometries are presented in Figure 4, and for sake of clarity, the geometries related to the breaking of the secondary interactions are not presented. Some key geometrical parameters are presented in Table 2.

In **7**, the geometry of the stannane adduct is somewhat different from the one found in **3**. Indeed, the stannane is interacting with the metal center through only one hydrogen atom (labeled H in Table 2), and no interaction is observed with Sn (La−Sn distance of 4.00 Å). Moreover, the C_3 axis of the remaining SnH_4 fragment of the stannane is oriented toward H. For the hydrostannyl complex moiety, the interaction between the metal and the ligand is still established through H′. Moreover, as can be seen from Tables 1 and 2, the hydrostannyl is not activated since the geometrical parameters are the same for **7** as for **5**. The C_3 axis of the hydrostannyl is still not oriented

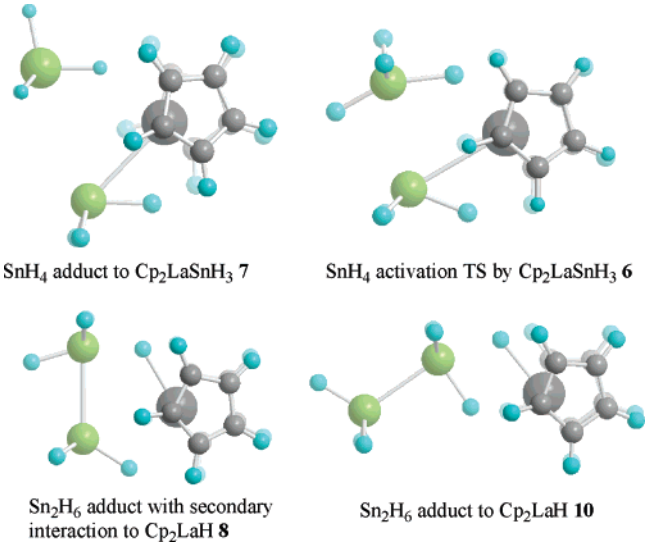

Figure 4. Optimized structures for the H/Sn exchange reaction.

Table 2. Selected Geometrical Parameters of the Stationary Points of the Second Step (bis-stannane formation by means of H/Sn exchange from hydrostannyl: $Cp_2LaSnH_3 + SnH_4 \rightarrow Cp_2LaH + Sn_2H_6$)

	7	6	8	10
La···H′ (Å)	2.43	2.56	2.57	6.16
La−Sn (Å)	3.24	3.24	3.29	5.78
La···H (Å)	2.49	2.25	2.23	2.21
La···Sn (Å)	4.00	3.71	3.70	3.57
Sn···Sn (Å)	4.18	3.16	3.05	2.87
H−Sn···Sn (deg)	70	85	88	162
H′−Sn···Sn (deg)	112	122	122	112

toward the metal center but to the incoming SnH_3 fragment. However, the Sn−Sn bond is not yet formed (distance of 4.18 Å). Thus, it can be concluded that this adduct does not efficiently prepare the transition state **6** since geometrical changes, such as reorientation of the C_3 axis of the incoming stannyl and the elongation of La−H′ bond, are necessary to reach the transition state **6**. A NBO analysis on **7** reveals that the negative charge on H′ has slightly decreased with respect to **5** (−0.40 vs −0.43), but the interaction is still important. At the same time, the charge on Sn(H′) has marginally increased (+0.13 vs +0.11), showing that the hydrostannyl is not much activated. For the incoming stannane, the situation is slightly different since the hydrogen that will be transferred to the metal center (H) is already negatively charged (−0.37) and Sn is positively charged (+0.93). This confirms that the interaction involves the hydrogen rather than Sn. Thus, adduct **7** can be viewed as a classic electrostatic adduct.

The geometry of the transition state **6** is rather different from that of the adduct **7**. Indeed, as can be seen from Table 2, the distance La···H′ has increased by 0.13 Å in order to decrease the interaction with the metal center. This decrease is also reflected by the increase of the bond angle H′−Sn···Sn. However, the interaction with the metal center is still present. Sn(H′) has not moved, since the C_3 axis was already oriented toward the incoming SnH_4, as shown by the La···Sn(H′) distance, which remains constant. At the same time, the stannane has come closer to the metal center, as described by the angle H−Sn−Sn, which has increased by 15°. The La−H bond is almost already formed (2.25 Å), as well as the Sn−Sn one (3.16 Å). The C_3 axis of the incoming SnH_3 has rotated but is not yet oriented toward the hydrostannyl group. This axis is oriented toward the metal center. However, a NBO analysis at the transition state does not reveal any interaction between Sn and

(33) Atheaux, I.; Delpech, F.; Donnadieu, B.; Sabo-Etienne, S.; Chaudret, B.; Hussein, K.; Barthelat, J.-C.; Braun, T.; Duckett, S. B.; Perutz, R. N. *Organometallics* **2002**, *21*, 5347.

the metal center, since the charge on Sn is still positive (+0.75). The interaction between H′ and La is confirmed by this analysis.

Indeed, the charge on H′ has decreased with respect to the adduct **7** but is still important (−0.34). The charge on H has increased to −0.47, revealing a stronger interaction. It should also be noticed that the charge on Sn(H′) has also increased with respect to the adduct (+0.34). The total charges of the two interacting SnH_3 fragments are +0.09 for the incoming SnH_3 and −0.38 for the hydrostannyl, explaining the bond formation.

The stabilization of the transition state by a secondary Sn−H interaction was confirmed by the NBO analysis. Thus, as one would expect from the nature of the transition state **6** and due to the fact that Sn has a tendency to stabilize anionic hypervalent states, it connects to complex **8**, where the two Sn−H interactions with the metal center are still present. A similar behavior was already reported in the case of silanes.[19] As can be seen from Table 2 and Figure 4, the geometry of **8** is very close to that of the transition state **6**. This is in agreement with the relatively low energetic stabilization of **8** with respect to **6**. The only major change is the decrease of the Sn−Sn bond distance by 0.11 Å, which seems to indicate a stronger interaction.

To form the adduct **10**, the system should reach the transition state **9**, which corresponds to a rotation around the Sn−Sn bond in order to reach a trigonal bipyramid geometry around $Sn^{\alpha}(H)$, with the hydride (H) occupying an apical position. Since, the rotation is not energy-demanding, it explains why the transition state **9** is only marginally destabilized with respect to **8** (0.3 kcal·mol^{-1}). The geometry of **10** keeps some features of the transition state **9** since the C_3 axis is still oriented toward the hydride. The geometry around Sn, which interacts with the hydride, is still a slightly distorted trigonal bipyramid. It should also be noticed that one of the hydrogens of the trigonal plane interacts with the metal center, leading to a stabilizing interaction. Moreover, the Sn−Sn bond distance has decreased to 2.87 Å, leading to a more covalent bond. Thus, this is in agreement with the stabilization of this adduct with respect to transition states **6** and **9**.

The entire process is thus calculated to be kinetically accessible for the stannane with the lanthanide catalyst. This mechanism was ruled out by Neale et al.,[6] with the smaller hafnium atom, based on steric hindrance around the metal center due to the size of the secondary stannane experimentally used, as well as the detection of cyclostannanes potentially yielded by cyclo-oligomerization of stannenes. The calculation of the transition state with four phenyl rings around the metal center is still complicated to achieve considering the size of the system, and so we have decided to only model the hindrance around the metal center by replacing only four hydrogen atoms by four phenyl rings on the optimized geometry of **6**. One should note that the geometry has been relaxed. As can be seen from Figure 5, no important steric effects can be observed, and thus, this pathway seems to be accessible with encumbered stannane, such as the one used by Neale et al.[6] This is clearly due to the size of the lanthanide center, which is very different from the hafnium used experimentally.

This pathway needs to be compared with the other possible pathway in order to check if it corresponds to the most kinetically accessible one. As all the pathways begin with the same first step, only the second step will be discussed in the following.

Stannylene Pathway: A Two-Step Pathway with Sn−H Activation and Stannylene Insertion into the Sn−H Bond. This pathway corresponds to the one proposed by Neale et al.[6] based on the experiment on the hafnium complex. The calculated free-energy profile is presented in Figure 6.

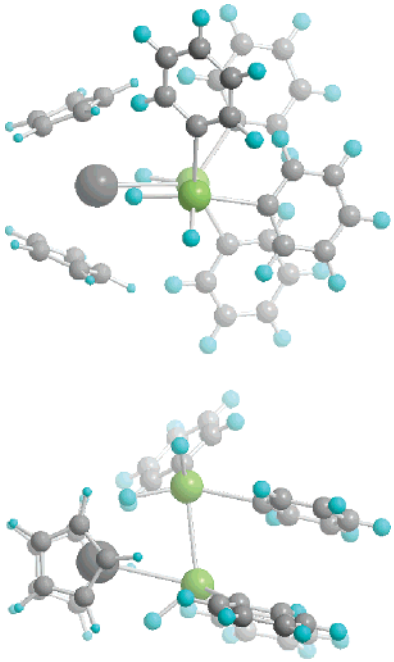

Figure 5. Model structures for **6** with SnH_2Ph_2.

Let us focus only on the second part of the free-energy profile, since the first part is the same as in the previously described pathway. First of all, as can be seen from Figure 6, this process is less favorable than the previously described one. Indeed, this process needs to reach two different transition states, **12** and **15**, which are calculated to be higher than the reference, respectively by +12.8 and +22.7 kcal·mol^{-1}. Thus, even if this process is kinetically accessible, the activation barriers obtained are significantly higher than the highest one obtained in the previous case by respectively 15.6 and 25.5 kcal·mol^{-1}. Thus, according to our calculations, this pathway is not competitive with the one previously described.

The first part of this second step consists in the formation and the release of the stannylene SnH_2. The formation of the stannylene from **5** is achieved by reaching the transition state **12** with an activation barrier of 31.1 kcal·mol^{-1} relative to **5** or 12.8 kcal·mol^{-1} relative to the reference **1**. The height of the activation barrier is associated with the important stability of the hydrostannyl complex **5** and also with the "stability" of the stannylene. However, this reaction is kinetically accessible, which is in agreement with the experiment done by Neale et al.[6] Thus, from **12**, it is not yet possible to release the stannylene SnH_2. Indeed, it should be noticed that the low "stability" of the free stannylene is observed by the formation of the adduct **13**, which is stabilized by 4.1 kcal·mol^{-1} with respect to **12**. From this adduct, it is possible to release the free stannylene. The stannylene **14** is found to be a singlet, which is more stable than the triplet one. The reaction is calculated to be endergonic by 30.4 kcal·mol^{-1} with respect to the hydrostannyl complex **5** and is very unlikely to occur. At this stage, it should be kept in mind that the intrinsic stability of the stannylene is very dependent on the choice of the stannane. In particular, it is clear that SnH_2 would be less stable than $SnMes_2$ (or $SnPh_2$) since the lone pair would be stabilized by electronic delocalization.[34] A calculation using SnH_2Ph_2 has been carried out, and the free energy of diphenylstannylene formation is calculated to be endergonic by 25.3 kcal·mol^{-1}, which is only 5.1 kcal·mol^{-1} less than for SnH_2. This value is in agreement with the fact the

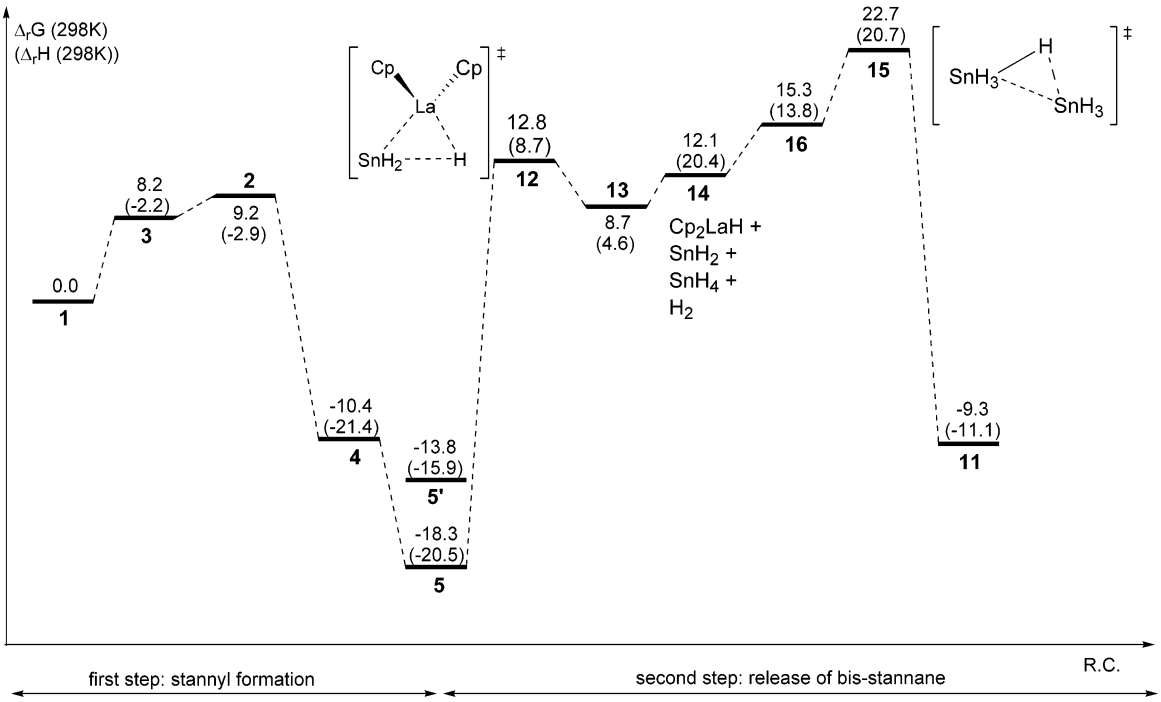

Figure 6. Free-energy profile of the "stannylene pathway". The free energies are given at 298 K, and the enthalpy values are in parentheses.

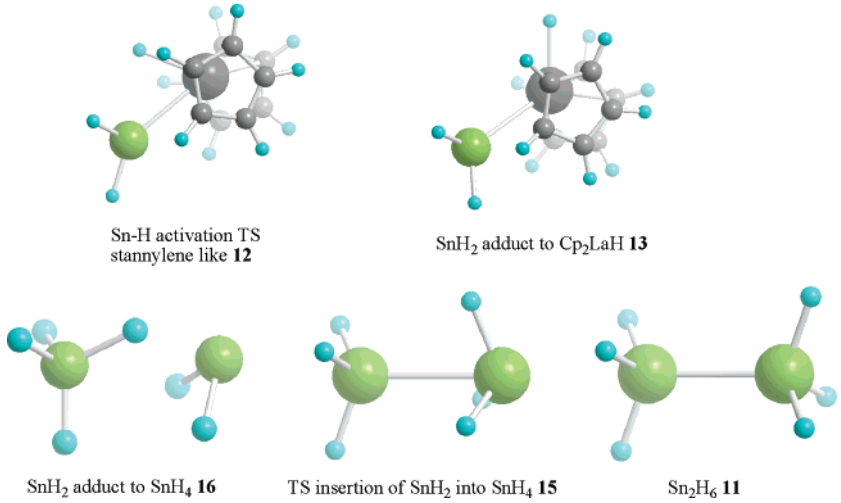

Figure 7. Optimized geometry of the stationary point of the "stannylene pathway".

free stannylene $SnPh_2$ is stabilized, but this small stabilization does not overcome the fact that the reaction is highly endergonic.

The second part of this second step corresponds to the insertion of SnH_2 into a Sn−H bond of SnH_4. This insertion begins by the formation of the adduct **16**, which is found to be destabilized by 3.2 kcal·mol^{-1}. This rather low destabilization can be explained by the fact that the adduct formation overcomes the low stability of the stannylene, but one still has to pay for the loss of entropy of SnH_2. Thus, the transition state **15** has to be reached. The activation barrier relative to the free stannylene **14** is calculated to be 10.6 kcal·mol^{-1}, which is 7.4 kcal·mol^{-1} above the adduct **16**. This value is in agreement with the one estimated by Trinquier:[21] 12.4 kcal·mol^{-1} at the MP_4 level of calculation. Thus **15** leads to the formation of the bis-stannane **11**.

The geometries of the optimized structures are presented in Figure 7. The geometry of the free stannylene is not included.

Table 3. Selected Geometrical Parameters of the Stationary Points of the Stannylene Formation

	12	**13**
La−H (Å)	2.20	2.14
La···Sn (Å)	3.19	3.31
Sn···H (Å)	2.92	4.82
H−Sn−H (deg)	95	96

Table 4. Selected Geometrical Parameters of the Stationary Points of the Stannylene Insertion

	16	**15**	**11**
Sn (stannylene)−H (bridging) (Å)	2.07	1.73	1.72
Sn (stannane)−H (bridging) (Å)	1.82	2.91	3.78
Sn···Sn (Å)	3.43	3.04	2.81
Sn···Sn−H (deg)	30	69	110

The key geometrical parameters are presented in Table 3 for the stannylene formation and in Table 4 for the insertion of the stannylene into the Sn−H bond. At the transition state **12**, the Sn−H bond is already broken (2.92 Å) and the hydride and the stannylene are already formed. It should be noticed that the

(34) Borden, W. T.; Gritsan, N. P.; Hadad, C. M.; Karney, W. L.; Kemnitz, C. R.; Platz, M. S. *Acc. Chem. Res.* **2000**, *33*, 765.

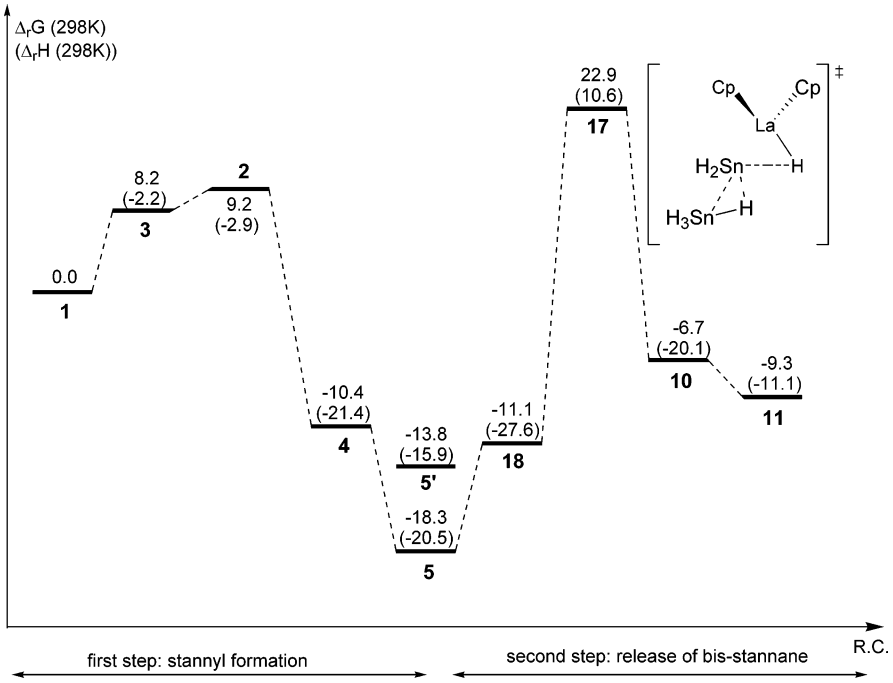

Figure 8. Calculated pathway for the stannylenoide-like reaction. The free energies are given at 298 K, and the enthalpy values are in parentheses.

H−Sn−H angle inside the stannylene is acute (95°). This geometry was already proposed by Trinquier[21] with an angle of 92.5° at the Hartree−Fock level. It should be noticed that in **12**, due to the low stability of the formed free stannylene, SnH_2 has moved above the equatorial plane, and one would expect an interaction with the electron-rich Cp ring. This was already observed in the case of carbene by Wekerma et al.[17] This situation is even more pronounced in the adduct **13**.

Indeed, it should be noticed that the stannylene is interacting with the Cp ring since one carbon atom is slightly pyramidal. This interaction stabilizes the complex and thus is in agreement with the low stability of the free stannylene. It should be noticed however that this kind of interaction would be unlikely to occur in the case of $SnMes_2$ or $SnPh_2$. Indeed, due to steric repulsion between the phenyl rings and the Cp ones, the stannylene would probably not interact with the Cp ring. Thus, it should be noticed at this stage that this is a difference between stannane and secondary stannane. For the stannylene insertion into the stannane molecule, the optimized geometries for stannylene−stannane complex **16** and the bis-stannane **11** are very standard and are in agreement with the results proposed in the literature.[21,35,36] However, the geometry of the transition state **15** is different; therefore, this geometry is discussed.

As can be seen from Figure 7 and Table 4, at the transition state, the Sn−Sn bond is almost formed (3.04 Å). Moreover, the hydrogen of the stannane that is bridging between the two interacting moieties is already transferred into the stannylene (Sn−H bond length of 1.73 Å). This geometry was the one proposed in the literature.[21] However, it should also be noticed that the remaining hydrogens on the stannylene are pointing in the direction of the incoming Sn atom. This is quite unexpected since it looks as if the hybrid sp^3 of the formed SnH_3 is pointing in the opposite direction of the other SnH_3. Thus, this seems not to be very stabilizing, explaining the height of the activation barrier with respect to the stannylene−stannane complex **16**. A NBO analysis at the transition state indicates that the three hydrogen atoms are negatively charged, whereas Sn is positively charged. Moreover, at the transition state, it should also be noticed that the SnH_3 coming from the stannane is positively charged (+0.10), whereas the other SnH_3, coming from the stannylene, is negatively charged (−0.10). Thus, this transition state is not stabilized by a covalent interaction but rather by an electrostatic interaction.

Thus, according to our calculation, this pathway seems to be unlikely to occur in order to produce bis-stannane if some stannane molecules are still present in the solution. This is mainly associated with the lower stability of the free stannylene with respect to the hydrostannyl complex. However, it should be noticed that from a kinetic point of view this reaction is accessible, and thus this reaction would certainly occur in the absence of stannane in the solution, leading to oligomerization of the free stannylene. Since this pathway is mainly unfavorable due to the formation of free stannylene, a concerted mechanism in which the stannylene is quenched by the incoming stannane consequently to its formation has been considered. This was proposed by Wekerma et al.[17] for carbenoide. This pathway would not imply the energy-demanding step of free stannylene release.

Stannylenoide Pathway: A Two-Step Pathway with Sn−H Activation and Stannylenoide Insertion into the Sn−H Bond. The calculated pathway is presented in Figure 8. As in the previous part on the free stannylene pathway, only the second step of the process is important. As can be seen from Figure 8, the process begins by the formation of the adduct **18**. This adduct is destabilized by 7.2 kcal·mol^{-1} with respect to the hydrostannyl complex **5**. This is in agreement with a loss of translational entropy of the stannane by coordination to the metal complex. Thus, for this adduct, one has to reach the transition state **17**, which lies 22.9 kcal·mol^{-1} above the reference, leading to an activation barrier of 41.2 kcal·mol^{-1} with respect to **5**. From a purely kinetic point of view, compared to the entrance channel, this reaction is still accessible. From the adduct, the activation barrier is calculated to be 34.0 kcal·mol^{-1}, leading

(35) Becerra, R.; Frey, H. M.; Mason, B. P.; Walsh, R.; Gordon, M. S. *J. Am. Chem. Soc.* **1992**, *114*, 2751.

(36) Fernandez-Sanz, J.; Marquez, A. *J. Phys. Chem.* **1989**, *93*, 7328.

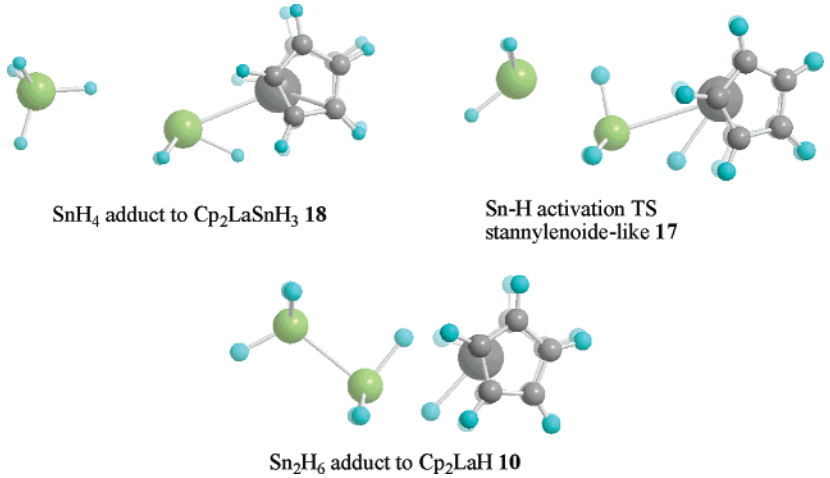

Figure 9. Optimized geometry of the stationary points for the stannylenoide pathway.

to the conclusion that the adduct does not efficiently prepare the transition state. Thus, **17** connects to the bis-stannane adduct **10**. Like the first process discussed, from **10** bis-stannane **11** is released.

As seen from Figure 8, the highest point in the free-energy pathway corresponds to the insertion of the stannyloide into the Sn−H bond of the stannane. It is noticeable that the value of +22.9 kcal·mol^{-1} is in excellent agreement with the value obtained for the insertion of the free stannylene into the Sn−H bond of the stannnane (+22.4 kcal·mol^{-1}). Thus, it can be concluded that the insertion of the stannylenoide into the Sn−H bond of the stannane is simply the same as the insertion of the free stannane and that the metal is not playing any role. This is confirmed by the geometry of the transition state **17**, presented in Figure 9.

Indeed, as can be seen from Figure 9, the geometry of the transition state **17** is very similar to the one described for the transition state **15**. The bridging hydrogen is already transferred to the stannylene, and the remaining hydrogens are pointing toward the incoming SnH_3. In that case, the explanation of why the sp^3 orbital is not pointing toward the incoming SnH_3 is more obvious since the hydride is still trans to the incoming SnH_3. Thus, the stannylenoide is still interacting with the hydride through an sp^3 orbital and the bis-stannane is stabilized by an electrostatic interaction. Since the geometries are very similar between transition state **15** and **17**, it is normal that the calculated activation barriers are similar. Thus, this pathway is similar to the one presented in the previous section, except that the endergonic formation of free stannylene is not necessary.

Conclusion

In this paper, the catalytic formation of bis-stannane in the presence of Cp_2LaH has been investigated by DFT. Rather than the secondary stannane used experimentally by Neale et al.,[6] the calculations were carried out with the simplest stannane SnH_4. Three different pathways leading to the bis-stannane formation have been investigated. All three pathways are two-step mechanisms starting with a common first step, which is the hydrostannyl formation by Sn−H activation. This step has been calculated to be exergonic by 18.3 kcal·mol^{-1}, and the formed hydrostannyl complex is stabilized by a Sn−H α-agostic interaction. A similar free energy of reaction has been obtained in the case of a secondary stannane, SnH_2Ph_2. The stability of the hydrostannyl complex is in agreement with the experiment by Neale et al.,[6] since the authors managed to crystallize this compound.

For the three pathways, the second step, leading to the bis-stannane formation and the regeneration of the catalyst, is calculated to be endergonic by 9.3 kcal·mol^{-1} with respect to the hydrostannyl complex. Thus, we can conclude at this stage that the second step is already under thermodynamic control. From a kinetic point of view, it has been demonstrated that all three pathways are kinetically accessible. The most kinetically accessible corresponds to an H/Sn exchange between the stannane and the hydrostannyl complex. This pathway is favored with respect to the other two by more than 25 kcal·mol^{-1}. A modeling of the nature of the transition state with the more bulky stannane (SnH_2Ph_2) shows that this transition state is not sterically destabilized. The pathway proposed by Neale et al.[6] with a hafnium catalyst based on the free stannylene formation is found to be less favorable in the lanthanide case, mainly due to the low stability of the free stannylene. To assess the influence of the metal center on the calculated pathway, the calculations are currently done with the hafnium-based catalyst. A similar behavior has been obtained with a more stabilized stannylene ($SnPh_2$). The stannylenoide pathway has been demonstrated to be similar to the stannylene pathway, since the metal plays no role in the insertion of the stannylenoide into the Sn−H bond of the stannane. The only difference is that in this pathway there is no need to release the free stannylene.

Thus, according to our calculations, one can conclude that the stannane mainly reacts with Cp_2LaH to form the hydrostannyl complex that accumulates. This is in agreement with the experimental results from Neale et al.,[6] since after 2 h, 64% of the metallic complex is hydrostannyl. Thus, a part of the hydrostannyl could react with stannane in an H/Sn exchange process to form bis-stannane and to regenerate the catalyst. After complete conversion of the stannane, the hydrostannyl can only decompose according to the free stannylene formation pathway. This leads to oligomerization of stannylene.

Acknowledgment. The authors are grateful to CINES and CALMIP for a grant of computer time.

Supporting Information Available: Table giving thermodynamic data and Cartesian coordinates of all optimized structures. This material is available free of charge via the Internet at http://pubs.acs.org.

OM051060M